Spur Decay of the Solvated Electron in Picosecond Radiolysis Measured with Time-Correlated Absorption Spectroscopy†

David M. Bartels,* Andrew R. Cook, Mohan Mudaliar, and Charles D. Jonah

Chemistry Division, Argonne National Laboratory, Argonne, Illinois 60439

Received: August 2, 1999; In Final Form: November 17, 1999

Spur decay kinetics of the hydrated electron following picosecond pulse radiolysis of water have been measured using a time-correlated transient absorption technique with an asynchronous mode-locked laser. The 11 ns time window afforded by this signal-averaging technique is ideal to match up with more conventional transient absorption measurements taken to microsecond time scales. The precise data recorded in this study require a revision downward of the "time zero" solvated electron yield to approximately 4.0 per 100 eV of energy absorbed, to match the best available scavenger product measurements.

Introduction

The practical importance of understanding radiolysis of water with fast electrons and γ radiation can hardly be overemphasized in fields such as radiation biology and nuclear engineering. Most of the details have been worked out for neat water near room temperature.[1−3] High-energy electrons and γ photons ionize molecules to produce low-energy secondary electrons, which proceed to ionize and electronically excite other molecules near the primary ionization site.

$$H_2O \xrightarrow{\gamma} e^- + H_2O^+ \quad (1)$$

The water radical cations immediately react with other water molecules to give (OH, H_3O^+) pairs. Secondary electrons quickly thermalize, trap, and become solvated electrons.

$$H_2O + H_2O^+ \rightarrow OH + H_3O^+ \quad (2)$$

$$e^- \rightarrow (e^-)_{aq} \quad (3)$$

Thus, well-separated clusters of ionization/excitation events (referred to as spurs) are generated on subpicosecond time scales, and diffusive recombination of the free radicals then occurs in competition with scavenging by other species in solution. The most important recombination reactions involve the dominant OH, H_3O^+, and $(e^-)_{aq}$ species:

$$(e^-)_{aq} + OH \rightarrow OH^- \quad (4)$$

$$(e^-)_{aq} + (e^-)_{aq} \rightarrow H_2 + 2OH^- \quad (5)$$

$$(e^-)_{aq} + H_3O^+ \rightarrow H + H_2O \quad (6)$$

$$OH + OH \rightarrow H_2O_2 \quad (7)$$

The effective yield of scavenged product—the chemical consequence of the radiation—depends on the scavenging rate constant and scavenger concentration (k_s[S], often referred to as scavenging power). If one knows the time-dependent survival probability of the primary radicals in neat solution, then one can predict scavenger product yields from the scavenging power. Similarly, through a Laplace transform relationship, the product yields vs scavenging power have been used to infer the time-dependent survival of the primary species.[4]

In a recent publication[5] a reexamination of the time-dependent yield of solvated electrons in radiolysis was undertaken to reconcile existing picosecond and nanosecond transient absorption measurements, scavenger yield measurements, and large-scale computer simulations. Upon reviewing older pulse radiolysis work, it was realized that stroboscopic kinetics measurements on the time scale 30 ps to 3 ns[6] and measurements using fast photodetectors on nanosecond and longer time scales[7] had never been carefully and convincingly matched together. Significant problems are the secondary response nonlinearities of fast-rise-time light detectors, and the limited time scale and drifts of the accelerator beam, which might distort the stroboscopic experiment based on Cerenkov probe light. The experiments reported here have been undertaken to provide a *fully linear* baseline measurement of the solvated electron kinetics for the time range 100 ps to 10 ns, following a 30 ps radiolysis pulse. To complete the study, kinetics were recorded with a fast digitizer/photodiode combination out to microsecond time scales. The new results show that the synthesis achieved in ref 5 was a reconciliation between several sets of flawed data.

Experimental Section

The experimental arrangement for picosecond radiolysis/time-correlated absorption spectroscopy is shown in Figure 1. The beam from a mode-locked Ti:sapphire laser is passed through a hole in the thick radiation shield wall, crosses a 1 cm flow cell in front of the 20 MeV electron beam (60 Hz, 30 ps pulses), and returns for detection by a Hamamatsu S5972 silicon photodiode. The basic idea is to measure absorption of the one laser pulse that arrives nearly coincident with the 30 ps electron pulse and to simultaneously measure the time delay between the electron and laser pulses. A histogram of absorption vs time events can then be constructed.

The long path traveled by the laser introduces 10−20% fluctuations in the light intensity, and a precise measurement of both transmitted and incident light is essential. The idea used here is that all fluctuations in intensity occur on a time scale

† Work performed under the auspices of the Office of Basic Energy Sciences, Division of Chemical Science, US-DOE under contract number W-31-109-ENG-38.

10.1021/jp992723e CCC: $19.00
Published on Web 02/05/2000

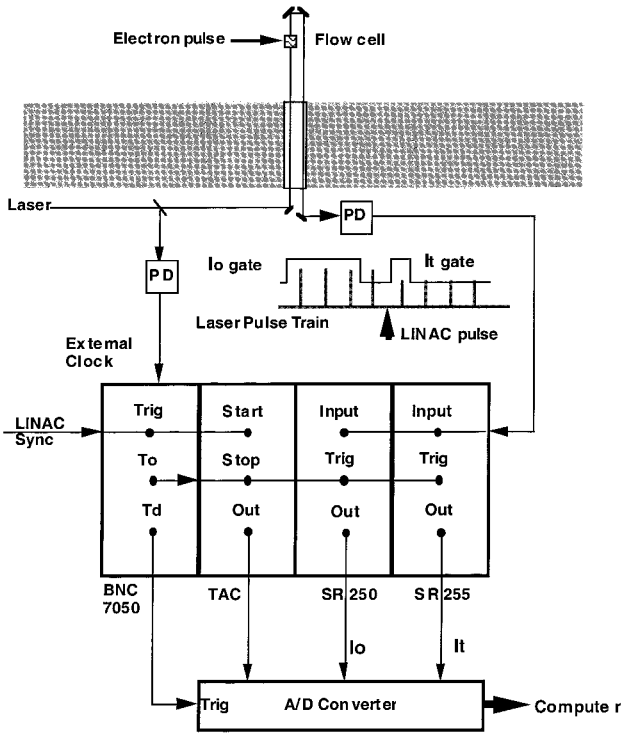

Figure 1. Schematic diagram for the time-correlated absorption measurement, as described in the text.

much longer than the 11 ns laser pulse spacing. Thus, we set the (I_t) gate of one gated integrator to measure the laser pulse nearly coincident with the electron pulse and the (I_o) gate of a second integrator to measure an average intensity of several pulses just prior to the electron pulse. The details of this arrangement are nontrivial. We first require a detector whose signal decays completely to baseline before the arrival of another laser pulse at the 90 MHz repetition rate. Second, a gating arrangement must be found that allows for two very fast high-precision measurements on the pulse train without distorting the information. We measure the single (I_t) pulse amplitude in a Stanford Instruments SR255 fast sampler with 1 ns gate width. This instrument is designed such that the fast signal is fed in and then out on 50 Ω cable, to be terminated in 50 Ω at the end of 2 m of cable. We use a feed-through 50 Ω termination, and measure an average intensity signal at this point with a high impedance (1000 Ω) operational amplifier circuit of 20 ns rise time. This signal is fed into a Stanford Instruments model SR250 gated integrator set to integrate a 60 ns window just before arrival of the electron pulse.

To provide triggers, a 90 MHz clock signal synchronous to the mode-locked Ti:sapphire laser is derived from a beam pickoff and photodiode. The photodiode signal is fed into a constant fraction discriminator, whose output is a very stable near-sine-wave used for the external clock of a BNC 7050 digital delay generator. A synchronization trigger from the Linac RF system arrives roughly 100 ns prior to the electron pulse. This pulse triggers both the BNC 7050 and the start of a time-to-amplitude converter (TAC). The prompt and delayed outputs of the BNC 7050 (now synchronized to the laser pulse train) are used to stop the TAC, and to trigger the two gated integrators for I_t and I_o measurement. For each incident electron pulse, a 12 bit A/D converter records the time delay (TAC) voltage and the I_t and I_o signals. On the basis of the TAC voltage, the I_t and I_o signals are summed into appropriate channels. The ratio I_t/I_o and the number of samples acquired in each channel is monitored as the experiment proceeds.

Sample solutions of ca. 300 mL volume were recirculated through the 1 cm square Suprasil flow cell using a Teflon/stainless steel gear pump, at a flow rate sufficient to replace the irradiated volume every two or three Linac shots. During the experiments argon was bubbled to remove oxygen, but no great precautions were taken to ensure sample purity given the short 10 ns time scale of measurement. All solutions were checked to ensure that the solvated electron lifetime was at least 1 μs before and after a run. Under these conditions no more than 1% of the initial signal can decay within 10 ns due to impurity scavenging or second-order chemistry, and the short-time spur kinetics of interest are minimally distorted. We were surprised to find that pure water gave typically a 300−500 ns electron lifetime at the 60 Hz repetition rate, while solutions of OH scavenger such as 0.1 M NaOAc or 0.02 M EtOH always gave a 1−3 μs lifetime or longer. We can only ascribe this observation to peroxide buildup in the flow cell due to inefficient flushing of some dead volume near the windows. The addition of even small amounts of hydroxyl radical scavenger greatly reduces the peroxide yield and lengthens the average electron lifetime.

At this point it is appropriate to comment on the advantages of the time-correlated absorption technique over other transient absorption methods. The first and most obvious advantage is the very high photon flux available with the laser-based probe light source. A stroboscopic technique based on Cerenkov light generated with part of the electron pulse has been used successfully for many years,[6] but the signal-to-noise ratio is limited by shot noise. Even worse, strong Cerenkov light generated in the sample inevitably is scattered into the detector, making signal/background very tiny in the UV spectral region. The implementation of this technique at Argonne has been limited to 3.3 ns full scale. A double pass delay stage might have been implemented to extend the time range, but alignment of the divergent Cerenkov light is difficult even for the 3.3 ns delay path. The Cerenkov light is also quite sensitive to the proper tune-up of the Linac itself, and any number of experiments failed due to poor initial tune or drifting over the course of a day. Because one is randomly collecting the entire kinetics window, time-correlated absorption is largely immune to any drifts of Linac operating parameters. Very fast transient digitizer/photodetector techniques have also been used over the years to obtain subnanosecond kinetics, but large corrections have to be made for the detector nonlinear response, and in general, one is always limited by shot noise. Time-correlated absorption spectroscopy has the advantage of complete linearity over whatever full scale is chosen (which could be any integer multiple of the laser repetition rate). For the first 10 ns of kinetics, time-correlated absorption is an ideal technique. On longer time scales, transient digitizer methods can be made more efficient.

To measure the spur decay at longer times, deoxygenated samples of neutral water from a Barnstead Nanopure cartridge system were irradiated with the same 30 ps Linac pulses in a 2 cm quartz cell. Transient absorption was recorded on a 1 μs time scale and longer using a Tektronix 645A digitizer with 250 MHz band-pass filter and 5 GHz sampling. Two detectors gave excellent agreement from 10 ns to longer time scales: an EG&G FND100 silicon photodiode with detection at 750 nm and a vacuum photodiode with detection at 600 nm. The light source was a 75 W xenon arc whose intensity was pulsed 50 to 100× for 300 μs for the measurement. Wavelengths were selected using 40 nm band-pass interference filters.

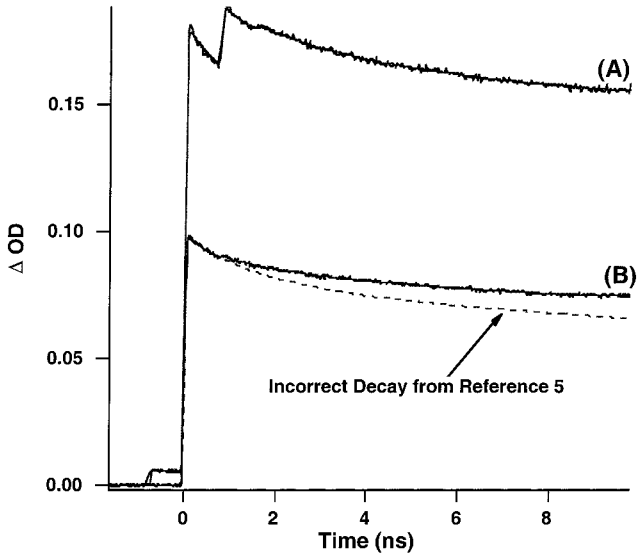

Figure 2. Transient absorption of solvated electron at 780 nm recorded following (A) full pulse and (B) half-charge Linac pulses. The solid-line fit curves include convolution with a Gaussian response function and include the time-shifted satellite pulses. The spur decay parameters fit to the half-charge pulse have been applied without modification to the full charge pulse. The dashed line indicates for comparison the incorrect result given in a recent publication.[5]

Results and Discussion

Figure 2 illustrates the quality of the raw data obtained in the laser experiment. The two traces shown represent transmission of a water sample following a full charge Linac pulse and a half-charge pulse. The full charge pulse has two clearly visible satellite pulses at ±760 ps. The half-charge pulse has one tiny satellite (typically 0.5%) following the main pulse. The ratio of I_t/I_o in the baseline was measured with a standard deviation of 0.5% per shot. The full 11 ns time scale was divided into 440 channels of 25.64 ps average width. Small corrections for the differential nonlinearity of the TAC were included in the fitting but made little difference. An average of 30 shots were recorded in each channel to produce the data illustrated here. At 60 Hz repetition rate of the Linac, this required some 4 min to acquire. A small amount of Linac RF noise was subtracted out by recording a dark baseline just before or just after the kinetics run. The rise time of the kinetics is ca. 100 ps, which must be limited by trigger jitter in the Linac/laser synchronization, because the Linac pulses are known to be 30 ps fwhm, and the 1 cm sample width should be too small to introduce this much distortion from walkoff of the electron and light beams (the relativistic electrons travel near the vacuum speed of light *c*, while the phase velocity of light in the water is *c* divided by the refractive index). Cross-correlation of the laser pulse train with itself, using a second BNC 7050 unit, demonstrated the electronics are capable of 12 ps time resolution.

Numerous cross-checks were made to ensure the signal was linear. A solution of 0.5 M $NaNO_3$ was used to check for transient absorption of the cell walls. The nitrate ion efficiently scavenges electrons both prior to and after their solvation, so this solution has only a tiny short-lived absorption at 780 nm. No change of the cell transmittance was detected after the electron pulse. The transient absorption in 0.1 M $HClO_4$ decayed to baseline with the time constant expected for the reaction of solvated electrons with hydronium ion.[8] Identical (but noisier) kinetics were obtained with half the laser intensity and, at other wavelengths, to check detector linearity.

TABLE 1: Fitting Parameters for Solvated Electron Spur Decay in the First Ten Nanoseconds[a]

solution:	A_1	T_1/ns	A_2	T_2/ns
water, 25 °C	0.1119	0.5195	0.2754	4.508
water, 6.5 °C	0.1370	1.1482	0.3308	9.361
water, 46 °C	0.2092	0.4200	0.3251	4.620
1.0 M ethanol	0.1081	0.5410	0.1807	5.090
0.1 M NaOAc	0.0909	0.5525	0.2350	4.079
0.1 M NaOH	0.0864	0.5451	0.1910	4.449
0.05 M NaOH	0.1436	0.5802	0.1928	5.669
0.01 M NaOH	0.1644	0.7513	0.1912	5.295
20% MeOH, 0.1 M NaOH	0.0772	0.2495	0.1200	5.128

[a] Fit equation: $1 + A_1 \exp(-t/T_1) + A_2 \exp(-t/T_2)$.

To fit the raw data, transient decays were described as the sum of two exponential functions plus a constant. The rise time was reproduced by convolution of this decay with a Gaussian function. To account for the satellite fine structure in the Linac pulses, data sets were represented by the sum of two or more of these functions, which were time-shifted relative to each other by 760 ns (known from the Linac RF frequency). Fitting parameters included the four (exponential) parameters needed to describe the kinetics shape, a time shift and a Gaussian width parameter to fit the signal rise, and individual scaling parameters for the charge in each fine structure pulse. The kinetics following both the full and half-charge Linac pulses were found to be identical after correction for the satellite pulses, as indicated by the almost invisible fit traces in Figure 2. In this example, the fundamental decay parameters were first obtained from the half-charge Linac data, which only requires a small correction for one satellite pulse. The fundamental decay parameters were then held fixed, and only the fine structure amplitude parameters were adjusted to fit the full-charge Linac pulse to well within the noise in the data. The exponential parameters found to describe multiple data sets in neat water at three different temperatures are reported in Table 1. (Note that these coefficients are only meant to represent the first 10 ns, as spur recombination continues out to hundreds of nanoseconds. The fit parameters have no mechanistic significance.)

In Figure 2, we have included for comparison the spur decay kinetics reconstructed from old data in ref 5. It can be seen that the new time-correlated absorption result disagrees with the reconstructed kinetics of ref 5, showing a substantially slower decay. The conclusions of ref 5 are, in fact, largely incorrect (see below). Reexamination of the stroboscopic absorption data used in ref 5 reveals that the best "clean" data set chosen to represent the first 3 ns for that publication was actually an outlier result with relatively fast decay. Other data sets from the Cerenkov light stroboscopic radiolysis experiment that have since been examined, including the original report in ref 6, agree very well with the first 3 ns of decay in the present study.

To check other results of ref 6, the effect of several concentrated scavengers on the spur kinetics were recorded and quantified. Results are illustrated in Figure 3, and the fit parameters are included in Table 1. As shown in ref 6, scavengers for either protons or hydroxyl radicals have a similar impact on the spur kinetics of solvated electrons, because solvated electrons react with both hydronium and hydroxyl with similar rate constants. The decay kinetics in 1.0 M ethanol and in 0.1 M NaOH are nearly identical on this time scale. A still longer electron lifetime is found in 1.0 M NaOH/25% methanol solution where both OH and hydronium ion are quickly scavenged. It was noted in ref 6 that concentrated hydroxide ion is more effective in preventing intraspur loss of solvated electrons than are other proton scavengers. Several effects must be considered in this comparison. First, the ionic strength effect

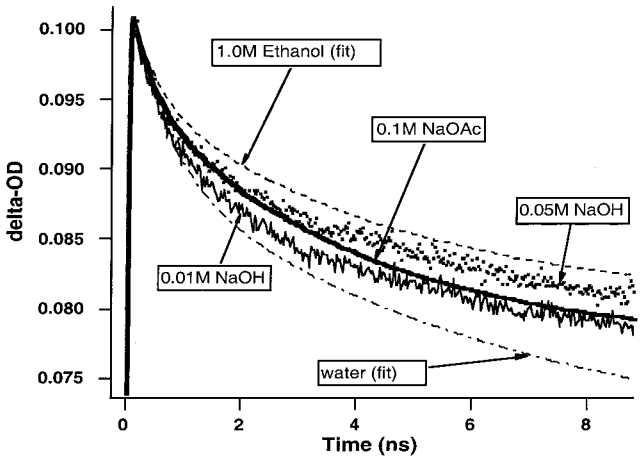

Figure 3. Transient absorption of solvated electron in several concentrated scavenger solutions following the half-charge Linac pulse. Raw data, corrected to remove the contribution of the 0.5% satellite pulse, are shown for the 0.01 and 0.05 M NaOH solutions. Normalized best-fit curves for the other solutions and pure water are superimposed for the sake of clarity.

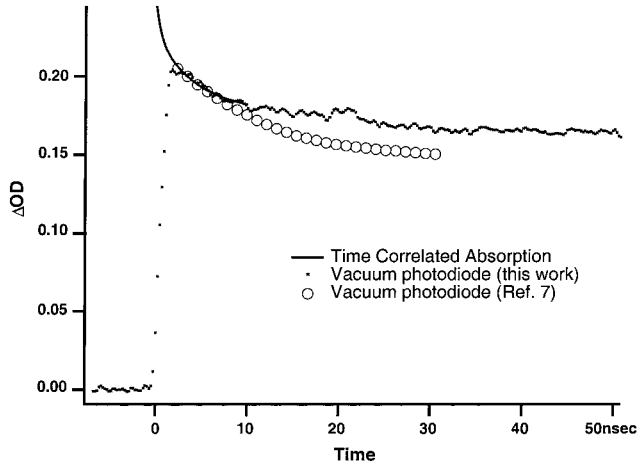

Figure 4. Matching of new vacuum photodiode/transient digitizer data (dots) with the result obtained from laser time-correlated absorption (line). Good matching of slopes is obtained between 3 and 10 ns. (The bump at ca. 20 ns is from a 1% reflection on the signal cable.) Old data from ref 7 recorded with the same vacuum photodiode (circles) are superimposed for comparison.

on reaction of ions will change both recombination rates and scavenging rates. Second, the ionic strength will alter diffusion rates of the ions, in particular slowing the diffusion of solvated electrons and hydronium ions. Finally, as a strong base the hydroxide ion will react with the hydroxyl radical, producing the oxide radical anion O^-. The anion reacts more slowly than the hydroxyl radical, both with itself and with solvated electrons.[3] Acetate and other weak bases do not effect this transformation. In Figure 3 we present data for 0.1 M acetate in comparison with 0.01 M NaOH and 0.05 M NaOH. The neutralization rate constant of acetate with hydronium ion is 4.5×10^{10} M^{-1} s^{-1}, while the hydroxide ion rate constant is[9] 1.4×10^{11} M^{-1} s^{-1}. In the 0.01 M NaOH solution, hydronium ions are scavenged in roughly 1 ns, while in the 0.05 M solution, hydronium is gone within several hundred picoseconds. In the acetate solution, after taking the primary ionic strength effect into account, the hydronium ion should be gone within ca. 500 ps. Hydrated electron kinetics in the acetate solution are intermediate between the two hydroxide solutions, but the slope is somewhat greater, especially at longer times. The difference seems to be qualitatively consistent with the OH/O^- equilibrium.

In ref 5 the (outlier) stroboscopic data were matched to an early study[7] of spur decay performed with a fast-rise vacuum photodiode and sampling oscilloscope that recorded kinetics from 200 ps to 35 ns. The splicing of data sets was performed by matching slopes at ca. 3 ns, on the assumption that secondary response nonlinearity distorted the vacuum photodiode data at earlier times. However, the new time-correlated absorption data reported here are not consistent with the older vacuum photodiode data. To extrapolate a solvated electron yield back to "zero" time, we made new measurements of the solvated electron absorption following our 30 ps pulse in a 2 cm Suprasil fused silica cell filled with Argon-bubbled water. In Figure 4 we show the first 50 ns of data recorded at 600 nm with the same vacuum photodiode used in ref 7. Superimposed is the (suitably scaled) fit of the time-correlated absorption data, whose slope matches the new digitizer data well from 3 to 10 ns. Also superimposed is the kinetic trace from ref 7, whose decay is clearly too fast. We have no explanation at this late date why ref 7 was incorrect. Perhaps the sampling oscilloscope used to record the data malfunctioned.

For quantitative analysis, data from an EG&G FND100 photodiode detector with 750 nm analyzing light was digitized every 200 ps out to 1 μs. (An identical but noisier result was obtained at 600 nm with the vacuum photodiode mentioned above.) We presume that all secondary response nonlinearities of these detectors have decayed away within 9 or 10 ns after the pulse. The slope of the laser time-correlated absorption data is consistent with these new transient digitizer measurements, as shown in Figure 4. The limiting lifetime of the solvated electron after the first 500 ns was ca. 5−10 μs for the first shot, limited by second-order recombination and some impurities (probably dominated by oxygen). The decay became progressively shorter as peroxide built up in the cell with each shot. To perform the most precise measurements, 5−15 shots were averaged, giving an average limiting lifetime of ca. 3−3.5 μs due to the peroxide. In the spirit of the isolated spur model[1−4] the survival of the hydrated electron in the presence of scavenger will follow the form

$$G(t) = G^\circ(t) \exp(-k_s[S]t) \tag{8}$$

where $k_s[S]$ is a scavenging rate. In the multiple shot experiment, the peroxide product acts as the dominant scavenger. The minor second-order homogeneous recombination can be subsumed into the "scavenger" exponential for fitting purposes.

To fit both the short time (laser) kinetics and the long time (lamp) kinetics at room temperature (25 °C), it was found necessary to use a functional form for $G^\circ(t)$ containing no less than four exponentials plus a constant:

$$G^\circ(t)/G_{inf} = 1 + 0.090 \exp(-t/139 \text{ ns}) + 0.128 \exp(-t/24.4 \text{ ns}) + 0.255 \exp(-t/3.51 \text{ ns}) + 0.118 \exp(-t/0.480 \text{ ns}) \tag{9}$$

The first 10 ns of the lamp/digitizer data were replaced by the (appropriately scaled) fit to the laser data, and then the combination was fit with the four-exponential sum, multiplied by a scaling factor and a "scavenging" exponential to fit the limiting decay. A good separation of spur and homogeneous kinetics is achieved because the "scavenging" time constant is greater than 3 μs, and the longest component of spur decay is 140 ns in this representation. Identical results are again obtained with the full and half-charge Linac pulses and in experiments run on several different days. By inspection of eq 9, the yield of hydrated electron at $t = 0$ is 1.59 times the escape yield

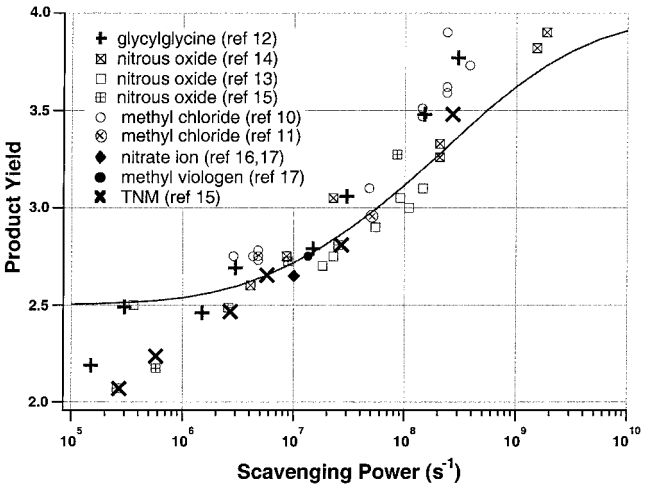

Figure 5. Comparison of experimental and predicted scavenged product yields, as a function of the scavenging power k_s[S].

G_{inf}. Perturbation of the fit parameters (e.g., forcing the longest time constant to 250 ns, then refitting the remaining parameters) suggests the ratio $G°(t=0)/G_{inf}$ must be correct to within about 3%. However, we have not carried out a formal sensitivity analysis.

Using this form for $G°(t)$ allows easy prediction of product yield in hydrated electron scavenger experiments by integration of eq 8 over time. In Figure 5 we plot this prediction as a function of k_s[S] together with product yield data for methyl chloride,[10,11] glycylglycine,[12] N_2O,[13−15] tetranitromethane (TNM),[15] nitrate,[16,17] and methyl viologen[17] scavengers. Taking $G_{inf} = 2.5$, we obtain $G(k_s[S]) = 2.7$ for a scavenging power of 1×10^7 s^{-1}, a result which the most precise scavenger studies have converged upon, with scatter of only 2−3%.[18] All of the scavenger results shown in Figure 4 lie within about 5−10% of the curve based on transient absorption, with residual scatter probably due to systematic errors in calibration. We consider the work of Elliot et al.[17] using both nitrate and methyl viologen scavengers, as perhaps the most reliable in the literature. Recent work of Buxton et al.[15] has shown good agreement for both N_2O and tetranitromethane scavengers. The precise methyl chloride measurement of Schmidt et al.,[11] which was based entirely on conductivity including a T-jump for dosimetry, is also in superb agreement with the predicted curve.

We should emphasize that we have not carried out any dosimetry in the present work. We have only measured the shape of the solvated electron decay, and used the integral over time to match the most reliable scavenger yields in Figure 5. Equation 9 accurately represents the data to produce random residuals of the fit from 100 ps to 1 μs, for several data sets collected on different days. The fitting parameters are not unique, in that covariance of individual exponential decay time constants and coefficients is significant. However, the basic shape of the $G°(t)$ decay is quite robust, independent of dose and scavenger (peroxide) concentration. The combination of laser and lamp transient absorption reported here almost certainly gives the correct ratio $G°(0)/G_{inf}$ to better than 5%, with most of the uncertainty in the lamp/digitizer data. Further cross-checks on the transient digitizer data could reduce this uncertainty.

The new extrapolated yield of $G°(0) = 4.0 \pm 0.2$ is significantly (ca. 20%) lower than the yield of 4.9 suggested in ref 5. As noted above, the previous number was based on erroneous old data, combined with the methyl chloride data[10] in Figure 4, which now appears to be about 10% high. The glycyl glycine data,[12] which seem to agree with ref 10, may be somewhat high at the largest concentrations used—glycine itself is known to scavenge electrons prior to solvation, which could inflate the product yield.[19] This effect of presolvated electron scavenging makes it essentially impossible to accurately determine $G°(t=0)$ by inverse Laplace transformation of the scavenger data,[4] and no doubt accounts for some of the scatter in the product yield literature.

Older numbers quoted for the solvated electron yield at 30 ps ($G°(30\text{ ps}) = 4.6$ in ref 6) were based on the dosimetry and the erroneously fast decay data in ref 7. The dosimetry used in ref 7 was based ultimately on the solvated electron extinction coefficient reported by Fielden and Hart,[20] which has since been shown to be 8% low.[21] (This correction alone would reduce the yield to 4.2 from 4.6.) The yield of $G°(30\text{ ps}) = 4.0$ estimated by Wolff et al.[22] referred to a limiting "microsecond" yield of 2.7 and so really should have been higher to agree with the present experiment.

It is worth noting that the often-cited estimate[23] of $G_{OH} = 5.9$ for the OH radical at 200 ps was based on an estimate of $G°(200\text{ ps}) = 4.5$ for the solvated electron. This number should apparently be reduced to $G_{OH}(200\text{ ps}) = 5.1$ on the basis of the present results.

At the low end of scavenging power, it must be recognized that the existence of an "escape" yield G_{inf} is an idealization based on the concept of isolated spurs in three dimensions. In reality, even low LET γ and electron radiation leaves a track of spurs, and ultimately in very low dose rate situations the diffusion of radicals will result in overlap of the spurs to form a diffuse track. (At a higher dose rate (i.e., track density), as in this study, diffusion may lead first to overlap of the separate tracks and a homogeneous concentration of species.) There is no diffusive escape ($G_{inf} = 0$) from a cylindrical track. The separation we have made between homogeneous chemistry and spur chemistry is entirely empirical and might well be slightly different if the dose per pulse in our experiment were reduced an order of magnitude or more. (Nevertheless very similar results have been found for the longest spur decay component using lower dose 2 ns electron pulses at the Notre Dame Radiation Laboratory.[24]) Some recent studies have called into question the utility of the G_{inf} idealization for low dose rate and low scavenger concentrations.[15,25] The very low scavenging power data of Buxton et al.[15] shown in Figure 5 could be matched by exchanging the constant 1 in eq 9 for an additional exponential decay with time constant of about 13 μs. Our time-resolved experiment is insensitive to such a slow component of track chemistry.

Conclusion

Using a new asynchronous laser sampling method we have measured the radiolysis spur recombination kinetics for the hydrated electron from 100 ps to 10 ns. These data were found to match up well at ca. 10 ns with new data collected with a transient digitizer and fast diode detectors. Fitting this combination of results gives a ratio of $G°(0)/G_{inf} = 1.59$ for an isolated spur model. Taking $G_{inf} = 2.50$ gives excellent agreement with product yield results of many scavenging experiments. The extrapolated "time-zero" hydrated electron yield is $G°(0) = 4.0 \pm 0.2$ electrons per 100 eV of deposited energy.

Acknowledgment. The authors would like to acknowledge Mr. Ed Kemereit for his contribution in operating and maintaining the Linac used in this work. We thank Dr. Richard Fessenden of the Notre Dame Radiation Laboratory for sharing unpublished data on the long-time component of spur decay,

and Dr. Craig Stuart of AECL for useful discussions. We also thank Drs. John Miller and Alexander Trifunac for their advice and encouragement in this work.

References and Notes

(1) Draganic, I. G.; Draganic, Z. D. *The Radiation Chemistry of Water*; Academic Press: New York, 1971.

(2) Farhataziz; Rodgers, M. A. J., Eds. *Radiation Chemistry. Principles and Applications*; VCH Publishers: New York, 1987.

(3) Buxton, G. V.; Greenstock, C. L.; Helman, W. P.; Ross, A. B. *J. Phys. Chem. Ref. Data* **1988**, *17*, 513.

(4) LaVerne, J. A.; Pimblott, S. M. *J. Phys. Chem.* **1991**, *95*, 3196.

(5) Pimblott, S. M.; LaVerne, J. A.; Bartels, D. M.; Jonah, C. D. *J. Phys. Chem.* **1996**, *100*, 9412.

(6) Jonah, C. D.; Matheson, M. S.; Miller, J. R.; Hart, E. J. *J. Phys. Chem.* **1976**, *80*, 1267.

(7) Jonah, C. D.; Hart, E. J.; Matheson, M. S. *J. Phys. Chem.* **1973**, *77*, 1838.

(8) Jonah, C. D.; Miller, J. R.; Matheson, M. S. *J. Phys. Chem.* **1977**, *81*, 931.

(9) Eigen, M.; Kruse, W.; Maass, G.; De Maeyer, L. *Prog. React. Kinet.* **1964**, *2*, 287.

(10) Balkas, T. I.; Fendler, J. H.; Schuler, R. H. *J. Phys. Chem.* **1970**, *74*, 4497.

(11) Schmidt, K. H.; Han, P.; Bartels, D. M. *J. Phys. Chem.* **1995**, *99*, 10530.

(12) Yoshida, H. *Radiat. Res.* **1994**, *137*, 145.

(13) Head, D. A.; Walker, D. C. *Nature* **1965**, *297*, 517.

(14) Dainton, F. S.; Logan, S. R. *Trans. Faraday Soc.* **1965**, *61*, 715.

(15) Buxton, G. V.; Lynch, D. A.; Stuart, C. R. *J. Chem. Soc., Faraday Trans.* **1998**, *94*, 2379.

(16) Haissinsky, M. *J. Chim. Phys.* **1965**, *62*, 1141.

(17) Elliot, J. A.; Chenier, M. P.; Ouellette, D. C. *J. Chem. Soc., Faraday Trans.* **1993**, *89*, 1193.

(18) A solvated electron radiolysis yield of 2.7 per 100 eV is often quoted in the literature without specifying 10^7 s^{-1} for the scavenging rate.

(19) Aldrich, J. E.; Bronskill, M. J.; Wolff, R. K.; Hunt, J. W. *J. Chem. Phys.* **1971**, *55*, 530. The C_{37} value reported for glycine is 5.6 M. If the same number applies to glycyl glycine, then at the highest concentrations (ca. 1 M) used in ref 12, approximately $4.0[1 - \exp(-1.0/5.6)] = 0.65$ G units of product could come from presolvated electron scavenging before any competition with recombination. This correction could put the results of ref 12 in substantial agreement with the predicted curve in Figure 5.

(20) Fielden, E. M.; Hart, E. J. *Trans. Faraday Soc.* **1967**, *63*, 2975.

(21) Elliot, A. J.; Ouellette, D. C. *J. Chem. Soc., Faraday Trans.* . **1994**, *90*, 837.

(22) Wolff, R. K.; Bronskill, M. J.; Aldrich, J. E.; Hunt, J. W. *J. Phys. Chem.* **1973**, *77*, 1350.

(23) Jonah, C. D.; Miller, J. R. *J. Phys. Chem.* **1977**, *81*, 1974.

(24) Dr. Richard Fessenden, Notre Dame Radiation Laboratory, personal communication.

(25) McCracken, D. R.; Tsang, K. T.; Laughton, P. J. Aspects of the Physics and Chemistry of Water Radiolysis by Fast Neutrons and Fast Electrons in Nuclear Reactors. AECL Report 11895; 1998.